Lamellar Branching of Poly(bisphenol A-*co*-decane) Spherulites at Different Temperatures Studied by High-Temperature AFM

Yong Jiang,† Da-Dong Yan, Xia Gao, Charles C. Han, Xi-Gao Jin, and Lin Li*

State Key Laboratory of Polymer Physics and Chemistry, Joint Laboratory of Polymer Science and Materials, Institute of Chemistry, Chinese Academy of Sciences, Beijing 100080, China

Yong Wang and Chi-Ming Chan*

Department of Chemical Engineering, Hong Kong University of Science and Technology, Clear Water Bay, Hong Kong

Received January 27, 2003; Revised Manuscript Received March 22, 2003

ABSTRACT: Thin films of poly(bisphenol A-*co*-decane) (BA-C10) were isothermally crystallized at different temperatures. The lamellar structures and branching during crystallization were observed in real time at different temperatures by an atomic force microscope equipped with a high-temperature heater accessory. Our observations indicated that induced nuclei developed into subsidiary lamellae, forming lamellar branches. Lamellar branches occurred randomly on the parent lamellae at high degrees of supercooling. However, lamellar branches were seldom observed at crystallization temperatures near the melting point. The minimum induction time for induced nucleation was found to occur at around 55 °C.

Introduction

Spherulites are common crystalline structures observed in melt-crystallized polymers. To account for spherulitic crystallization, one must explain the origin of profuse lamellar branching. Keith and Padden[1,2] suggested that bundles of discrete fibers are formed based on the observations using a polarized optical microscope. By extending the technique of permanganic etching developed for electron microscopy, Bassett et al. investigated the lamellar morphologies of melt-crystallized isotactic polystyrene (*i*-PS) and isotactic polypropylene (*i*-PP) in details.[3−6] They proposed that the skeleton of a spherulite is established by individual dominant lamellae that branch and splay apart, leaving interstices to be filled by later-crystallizing subsidiary lamellae. The pressure built up by molecular cilia between the dominant lamellae induces lamellar splaying. Lamellar branching is mainly induced through giant screw dislocations. In addition, they concluded that the subsidiary lamellae contain shorter molecules on average than do the dominant ones. At the same time, Norton and Keller studied the basic morphology of melt-crystallized i-PP.[7,8] Their investigations focused on five different spherulitic types, as identified by optical microscopy. Their results suggested that each spherulitic type is characterized the arrangement of its constituent lamellae in terms of orientation, habit type, and crystal structures. Lamellar crosshatch, namely lamellar branching, involves some form of "pure" epitaxy (i.e., a process that is related to some fundamental lattice constant rather than a method of branch propagation by the deposition of an intermediate γ-phase). Despite many studies on this topic, our current understanding of morphology does not give us a comprehensive understanding of lamellar branching of melt-crystallized polymers.

In recent years, studies of polymer crystallization using atomic force microscopy (AFM) have attracted considerable interest due to the unique combination of the techniques's high-resolution and real-time features. In particular, tapping-mode AFM with the phase imaging function substantially complements optical microscopy with its high-resolution and also complements transmission electron microscopy (TEM) because it can be used under ambient conditions and does not need special sample treatment. Tapping-mode AFM has been used to study the lamellar structures of various semicrystalline polymers.[9−27]

As we previously reported,[9−12] real-time investigations of the growth processes of lamellae and spherulites of poly(bisphenol A-*co*-alkyl ether) using AFM suggested that a lamella breeds more lamellae via induced nucleation. The branching of parent lamellae is a result of the growth of induced nuclei into subsidiary lamellae.[9,10] We proposed that the polymer chains that were partially trapped in the parent lamellae could easily adjust their conformations to form induced nuclei near their parents. In this work, the influences of crystallization temperature on the formation of induced nuclei were investigated. The branching of lamellae at different temperatures was studied by AFM in real time.

Experimental Section

Poly(bisphenol A-*co*-decane) (BA-C10) was prepared as described previously.[9−12] The glass transition temperature, melting point, weight-average molecular weight, and polydispersity index were measured to be 10.5 °C, 95 °C, 29 480 g/mol, and 2.6, respectively. Thin films for AFM observation were prepared by spin-coating 10−20 mg/mL polymer−chloroform solutions at 3000 rpm onto the surface of freshly cleaved mica samples. The film thickness was measured to be approximately 100−150 nm using AFM. The influence of the substrate on the lamellar branching behavior can be neglected when the film thickness is above 100 nm. Dewetting of films did not

† Present address: Graduate School of the Chinese Academy of Sciences.

* To whom correspondence should be addressed. E-mail: lilin@iccas.ac.cn.

10.1021/ma0341061 CCC: $25.00
Published on Web 04/25/2003

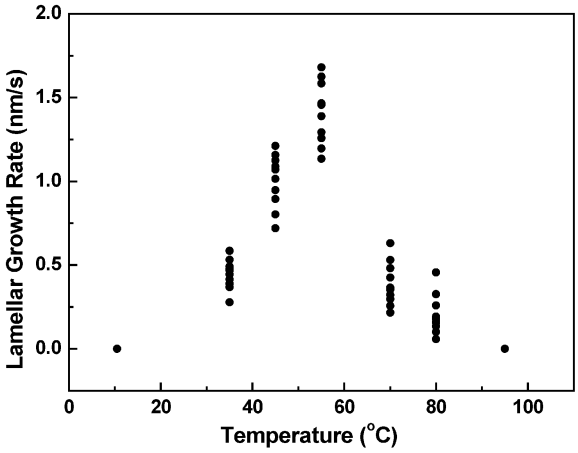

Figure 1. Lamellar growth rate as a function of crystallization temperature T_c determined by AFM.

occur even at elevated temperatures, such as at 120 °C. The film was heated to 120 °C for 10 min to melt the crystal phase and then quenched to a chosen crystallization temperature for AFM observations. Tapping-mode AFM images were obtained using a NanoScope III MultiMode AFM (Digital Instruments) equipped with a high-temperature heater accessory (Digital Instruments). The measured temperature ranging from 25 to 95 °C of the AFM hot-stage was calibrated using a thermocouple held to the mica surface by a magnetic sheet. It has been shown that the measured surface temperature of a thin film of poly(ethylene oxide) with a thickness of 130 nm was overestimated by 0.1 °C at surface temperature of 57 °C.[24] Large temperature errors were found for films with a thickness in the tens of micrometers. Therefore, in the current study, the relative temperatures for polymer films with a thickness of about 150 nm should be comparable. The experimental details of high-temperature AFM can be found in everywhere.[13−26] Both topographic and phase images were recorded simultaneously, and only the AFM phase images are presented. Si cantilever tips (TESP) with a resonance frequency of approximately 300 kHz and a spring constant of about 40 N m^{-1} were used. The scan rate varied from 0.5 to 1.5 Hz. The typical value for the amplitude was 2.0 V, and the set point amplitude ratio ($r_{sp} = A_{sp}/A_o$, where A_{sp} is the set-point amplitude and A_o is the amplitude of the free oscillation) was adjusted to 0.7 to 0.9. The amplitude and set-point ratio were chosen such that the surface was tracked while maintaining the necessary contrast in the phase images. The lamellar thickness was obtained by the section analysis using AFM images with a scan size less than 1 μm × 1 μm.

Results and Discussion

Figure 1 shows the lamellar growth rate as a function of the crystallization temperature of the BA-C10 polymer. The maximum lamellar growth rate occurred at around 55 °C. It should be noted that the lamellar growth rates are very small. This allows an in-situ study of the growth and branching of lamellae at different crystallization temperatures using AFM. Figure 2 shows the AFM phase images of the lamellar branches developed at 35, 55, 70, and 75 °C. At about 35 °C, the branches were arranged fairly irregularly, as shown in Figure 2a. The detailed statistic results showed that the subsidiary lamellae had almost the same growth rates as the dominant lamellae. However, the lengths between the branch points and the tips of the subsidiary lamellae were approximately 200−500 nm shorter than the lengths between the branch points and the tips of the parent lamellae, as indicated by arrows in Figure 2a. At 55 °C, it was difficult to distinguish between the dominant and subsidiary lamellae (cf. Figure 2b). In this

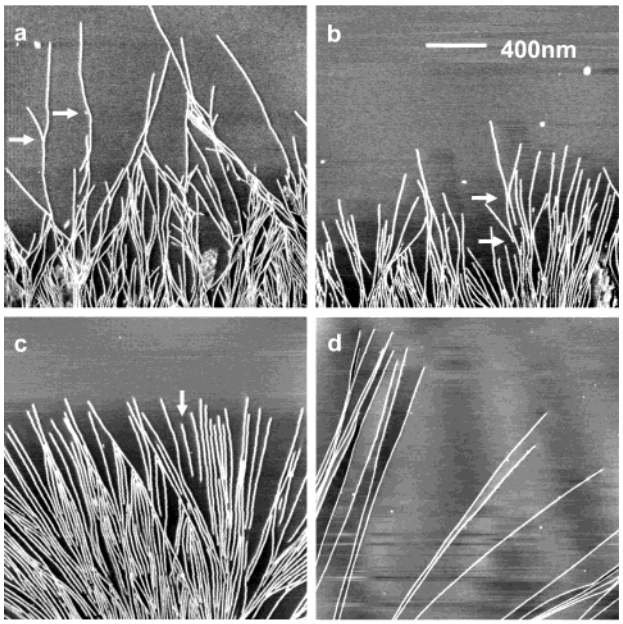

Figure 2. AFM phase images of lamellae of the BA-C10 spherulites crystallized at (a) 35, (b) 55, (c) 70, and (d) 75 °C.

case, the lengths between the branch points and the tips of the subsidiary lamellae were only 50−150 nm shorter than the lengths between the branch points and tips of the parent lamellae. At 70 °C, the number of lamellar branches was very small, and the subsidiary lamellae were orderly and aligned almost parallel to the dominant lamellae as shown by the arrow in Figure 2c. Some branching occurred almost at the tips of the dominant lamellae. It was difficult to determine whether they were generated from induced nuclei or primary nuclei. Branching was not observed at 75 °C, and the lamellae grew very straight, as shown in Figure 2d. A comparison of the phase images of the lamellar branching shown in Figure 2 indicates that the thickness of the lamellae grown at 70 and 75 °C appeared to be larger than that of the lamellae developed at 35 and 55 °C. The statistical results by section analysis using an AFM software showed that the average widths of the lamellae crystallized at 35, 55, 70, and 75 °C were about 8, 10, 11, and 12 ± 2 nm, respectively. Quantitative measurements at temperatures above 75 °C were difficult because high-quality images could not be obtained. In addition, the thickening effect of the lamellae at high temperatures could not be accurately measured because of the broadening effects caused by different AFM tips and different set-point amplitude ratios. However, we were certain that the dominant and subsidiary lamellae formed at the same crystallization temperature showed no significant difference in the average width.

Figure 3 shows two founding lamellae with a few lamellar branches developed at 35 and 55 °C. At the initial stage of the lamellar growth, the distance between a lamellar branch and the growing tip of a founding lamella varied with crystallization temperature. Most recently, we found that various types of lamellar branching can be caused by the defects artificially induced by an AFM tip through adjusting the AFM set-point amplitude ratio.[27] By adjusting the AFM set-point amplitude ratio to ensure that the AFM was operated in the light-tapping mode, the effects of the AFM tip on lamellar branching and nucleation could be neglected.[11,16,21] Our results clearly indicated that lamel-

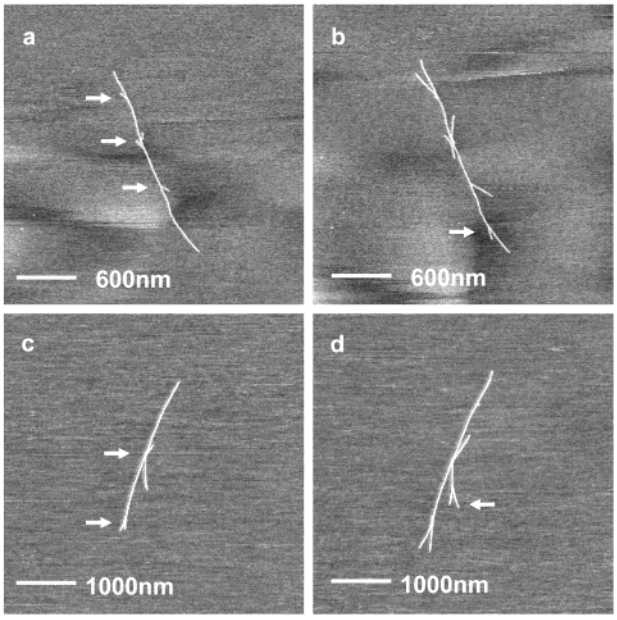

Figure 3. AFM phase images showing the branching of a founding lamella at 35 °C (a, b) and at 55 °C: (c, d). The time interval between (a) and (b) was 6 min and between (c) and (d) was 5 min.

lar branches developed from induced nuclei of the parent lamellae. The polymer chains that were partially trapped in the parent lamellae could easily adjust their conformation to form induced nuclei near the parent lamellae. In fact, a number of computer simulations have suggested that chain stiffness of a semicrystalline polymer might significantly influence the concentration of loose loops or cilia at the lamellar surface.[28−31] Some protruding cilia or partially trapped polymer chains with a similar conformation could easily form induced nuclei near the folding surface of a parent lamella. The protruding cilia or trapped polymer chains with different conformations could still adjust and rearrange to form induced nuclei but after much longer time. Therefore, the first induced nucleus is often observed to appear near the center of a founding lamella, as indicated by the arrows in Figure 3.

Figure 4a is a schematic showing branching of a founding lamella—v is the average growth rate of the lamella and L_0 is the length between the lamellar tip and the location at which an induced nucleus just appeared. According to our observations, the growth rates of the founding lamella were quite uniform with time at a given crystallization temperature. Thus, we define the induction time, t_i, for the formation of an induced nucleus by

$$t_i = \frac{L_0}{v} \tag{1}$$

However, it is difficult to measure L_0, while in most cases, L_1 and L_1', as defined in Figure 4a, could be obtained easily when a subsidiary lamella grew to a certain length. Thus, the induction time is given by

$$t_i = \frac{L_0}{v} = \frac{L_1 - L_1'}{v} \tag{2}$$

The induction time was calculated using the measured values of L_1, L_1', and v for the founding and subsidiary lamellae. The reported value was an average

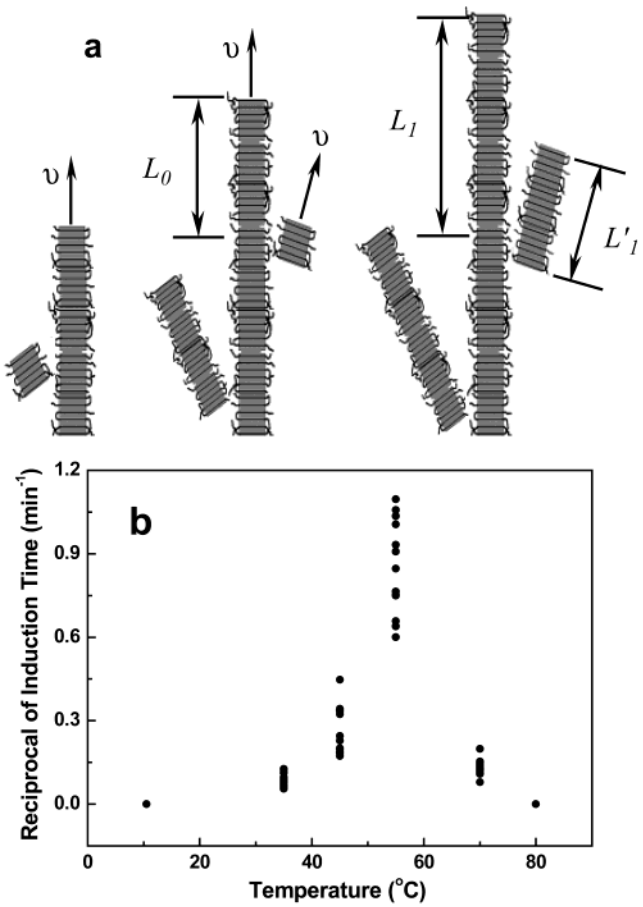

Figure 4. (a) A schematic drawing illustrating the branching of a founding lamella and (b) a plot of the reciprocal of induction time, t_i, for subsidiary lamellae as a function of crystallization temperature.

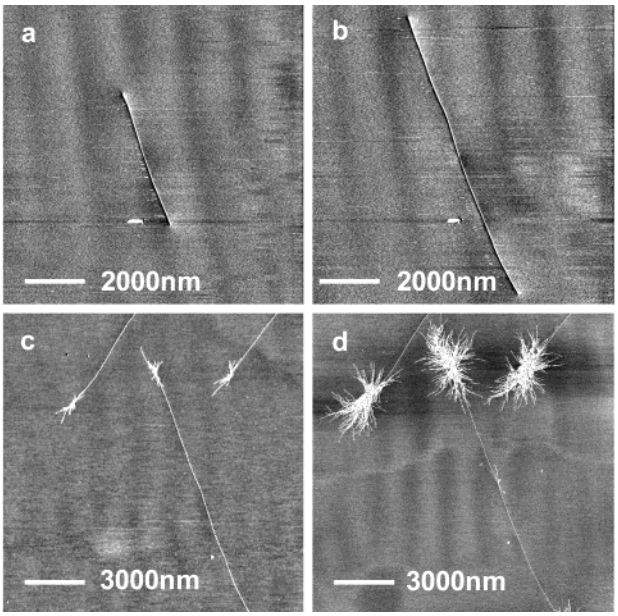

Figure 5. In-situ phase images showing the lamellar branching at different temperatures: (a, b) no branching at 80 °C; (c, d) branching largely at the tips of lamellae when the temperature was quenched to 35 °C.

of 10−15 measurements. The minimum in the plot of t_i as a function of crystallization temperature was determined to be at about 55 °C, which is the same as the temperature at which maximum lamellar growth rate

occurs. As seen in Figure 4b, induction time was quit long when the crystallization temperature was lower than about 35 °C. Thus, induced nuclei hardly formed and the number of lamellar branches was very small at this temperature. It is important to state that when the crystallization temperature was higher than 75 °C, induced nuclei also did not form. As a result, subsidiary lamellae were mostly absent and spherulites could not form above this temperature. But other factors such as impurities could still promote the formation of primary nuclei. Hence, at this temperature, a heterogeneous nucleus could grow into a single crystal. Our recent observations suggest that at about 75−80 °C flat-on lamellae or hedrites can still be formed in thin films with thickness less than 100 nm. The detailed discussion of this subject will be presented in a forthcoming paper.

It is easy to understand that at low crystallization temperatures the lamellar branching rate is small because the adjustment of the chain conformations is limited due to the immobility of these partially trapped chain segments. At high crystallization temperatures near the melting point, the driving force for secondary nucleation decreases, resulting in lower growth rates of the lamellae. The reduction in the induced nucleation rate at high temperatures is due to the fact that the increased thermal mobility of polymer chains and the small secondary nucleation rate provide enough time for the polymer chains to adjust their conformations to fold into a lamella with few protruding cilia or partially trapped chain segments. As a result, lamellar branching seldom occurs at high crystallization temperatures. A perfect edge-on lamellar single crystal without any branches developed at 80 °C (T_m = 95 °C) and grew to 20 μm long, as shown in Figure 5a,b. However, when the temperature was quenched to 35 °C, many lamellar branches appeared at the growing tips of this single long lamella, as shown in Figure 5c,d. The reason why it was very difficult to form induced nuclei and lamellar branches at the center part of this single lamella is because this lamella developed at 80 °C with possibly no defects such as protruding cilia or trapped chain segments.

Conclusions

Lamellar branching during the formation processes of BA-C10 spherulites was studied by AFM in real time at different crystallization temperatures. It was found that lamellar branching follows different patterns at different temperatures. Lamellar branches generated irregularly at 35 °C, and straight dominant and subsidiary lamellae developed at high temperatures. The minimum induction time for lamellar branching was found to occur at the crystallization temperature of 55 °C. Edge-on lamellae that developed around 70 °C were straight with only a few branches. Our observations suggested that induced nuclei hardly form at crystallization temperatures above 70 °C. The induction time for lamellar branching can be determined by AFM.

Acknowledgment. We are grateful for the support of National Science Foundation of China (Grants 20044005 and 20174049), Hong Kong Government Research Grants Council under Grant 6176/02P, and the National Science Foundation of China and the Hong Kong Government Research Grants Council Joint Research Scheme under Grants NSFC 20131160730 and N_HKUST 618/01.

References and Notes

(1) Keith, H. D.; Padden, F. J. *J. Appl. Phys.* **1963**, *34*, 2409.
(2) Keith, H. D. *J. Polym. Sci., Part A* **1964**, *2*, 4339.
(3) Bassett, D. C. *Principles of Polymer Morphology*; Cambridge University Press: Cambridge, 1981.
(4) Bassett, D. C.; Keller, A.; Mitsuhashi, S. *J. Polym. Sci., Part A* **1963**, *1*, 763.
(5) Bassett, D. C.; Olley, R. H. *Polymer* **1984**, *25*, 935.
(6) Bassett, D. C.; Vaughan, A. S. *Polymer* **1985**, *26*, 717.
(7) Norton, D. R.; Keller, A. *J. Mater. Sci.* **1984**, *19*, 447.
(8) Norton, D. R.; Keller, A. *Polymer* **1985**, *26*, 704.
(9) Li, L.; Chan, C. M.; Li, J. X.; Ng, K. M.; Yeung, K. L.; Weng, L. T. *Macromolecules* **1999**, *32*, 8240.
(10) Li, L.; Chan, C. M.; Yeung, K. L.; Li, J. X.; Ng, K. M.; Lei, Y. G. *Macromolecules* **2001**, *34*, 316.
(11) Lei, Y. G.; Chan, C. M.; Li, J. X.; Ng, K. M.; Jiang, Y.; Li, L. *Macromolecules* **2002**, *35*, 6751.
(12) Jiang, Y.; Gu, Q.; Li, L.; Shen, D. Y.; Jin, X. G.; Lei, Y. G.; Chan, C. M. *Polymer* **2002**, *43*, 5615.
(13) Hobbs, J. K.; McMaster, T. J.; Miles, M. J.; Barham, P. J. *Polymer* **1998**, *39*, 2437.
(14) Pearce, R.; Vancso, G. J. *Polymer* **1998**, *39*, 1237.
(15) Pearce, R.; Vancso, G. J. *J. Polym. Sci., Polym. Phys.* **1998**, *36*, 2643.
(16) Beekmans, L. G. M.; Vansco, G. J. *Polymer* **2000**, *41*, 8975.
(17) Ivanov, D. A.; Nysten, B.; Jonas, A. M. *Polymer* **1999**, *40*, 5899.
(18) Basire, C.; Ivanov, D. A. *Phys. Rev. Lett.* **2000**, *85*, 5587.
(19) Ivanov, D. A.; Amalou, Z.; Magonov, S. N. *Macromolecules* **2001**, *34*, 8944.
(20) Magonov, S. N.; Godovsky, Y. *Am. Lab.* **1999**, *31*, 52.
(21) Godovsky, Y. K.; Magonov, S. N. *Langmuir* **2000**, *16*, 3549.
(22) Fasolka, M. J.; Mayes, A. M.; Magonov, S. N. *Ultramicroscopy* **2001**, *90*, 21.
(23) Frank, C. W.; Rao, V.; Despotopoulou, M. M.; Pease, R. F. W.; Hinsberg, W. D.; Miller, R. D.; Rabolt, J. F. *Science* **1996**, *273*, 912.
(24) Schönherr, H.; Bailey, L. E.; Frank, C. W. *Langmuir* **2002**, *18*, 490.
(25) Schönherr, H.; Frank, C. W. *Macromolecules* **2003**, *36*, 1188.
(26) Schönherr, H.; Frank, C. W. *Macromolecules* **2003**, *36*, 1199.
(27) Wang, Y.; Chan, C. M.; Ng, K. M.; Jiang, Y.; Li, L.; Lei, Y. G.; Cheung, Z.-L. Manuscript in preparation.
(28) Kumar, S. K.; Yoon, D. Y. *Macromolecules* **1989**, *22*, 3458.
(29) Yoon, D. Y.; Ando, Y.; Rojstaczer, S.; Kumar, S. K.; Alfonso, G. C. *Macromol. Symp.* **1991**, *50*, 183.
(30) Kumar, S. K.; Yoon, D. Y. *Macromolecules* **1991**, *24*, 5414.
(31) Ivanov, D. A.; Pop, T.; Yoon, D. Y.; Jonas, A. M. *Macromolecules* **2002**, *35*, 9813.

MA0341061